

ULUSLARARASI 3B YAZICI TEKNOLOJİLERİ
VE DİJİTAL ENDÜSTRİ DERGİSİ

INTERNATIONAL JOURNAL OF 3D PRINTING
TECHNOLOGIES AND DIGITAL INDUSTRY

ISSN:2602-3350 [Online]

URL: <https://dergipark.org.tr/ij3dptdi>

EVALUATION OF THE PROCESS PARAMETER AND PERFORMANCE OF L-DED SS316L-IN718 BIMETALLIC STRUCTURES

Yazarlar (Authors): Mustafa Kaş^{ID}*, Oğuzhan Yılmaz^{ID}



Bu makaleye şu şekilde atıfta bulunabilirsiniz (To cite to this article): Kaş M., Yılmaz O., “Evaluation of the Process Parameter and Performance of L-DED SS316L-In718 Bimetallic Structures” *Int. J. of 3D Printing Tech. Dig. Ind.*, 9(2): 263-271, (2025).

DOI: 10.46519/ij3dptdi.1700837

Araştırma Makale/ Research Article

Erişim Linki: (To link to this article): <https://dergipark.org.tr/en/pub/ij3dptdi/archive>

EVALUATION OF THE PROCESS PARAMETER AND PERFORMANCE OF L-DED SS316L-IN718 BIMETALLIC STRUCTURES

Mustafa Kaş^a , Oğuzhan Yılmaz^a 

^a Advanced Manufacturing Technologies Research Group (AMTRG), Mechanical Engineering Department, Faculty of Engineering, Gazi University, TURKEY

* Corresponding Author: mustafakas@gazi.edu.tr

(Received: 16.05.25; Revised: 11.06.25; Accepted: 01.07.25)

ABSTRACT

Laser Direct Energy Deposition (L-DED) is a promising additive manufacturing technique with potential application in joining two dissimilar materials to fabricate bi-metallic components. The quality and functionality of the bonding interfaces are of great significance and rely heavily on the process parameters. In this work, we first deposited IN718 on a wrought SS316L substrate to create a bimetallic interface. Different energy density values, ranging from 71.43 to 127.7 J/mm, were used through various combinations of laser power and scanning speed for deposition. The bimetallic interface quality in terms of interface geometry, morphology, and dilution values was investigated for every energy density. Geometric analyses and dilution measurements revealed that the optimum bimetallic fabrication was achieved with an energy density of 90–100 J/mm. To deposit bimetallic SS316L-IN718 blocks for mechanical testing, the laser power and scan speed were set to 1400 W and 14 mm/s, respectively. Line EDS measurements revealed a transition zone across the bimetallic interface within a 4 mm distance, avoiding abrupt chemical discontinuities. Micro-hardness testing using Vickers revealed a smooth hardness transition between the SS316L (~210 HV) and IN718 (~300 HV) sides without any defect formation, suggesting successful joining. The bimetallic structure exhibited yield strength of 268.88 ± 20 MPa, tensile strength of 462 ± 12 MPa, and elongation of $19.6 \pm 0.8\%$, in good agreement with SS316L. The fracture occurred on the SS316L side with noticeable necking and ductile behavior, demonstrating good interfacial bonding. These findings demonstrate the potential of L-DED in the fabrication of bimetallic structures for structural applications.

Keywords: L-DED, Bi-Metal, SS316L, IN718

1. INTRODUCTION

The demand for complex and multi-functional materials has been increasing as technology advances. This need has driven the exploration of multi-material structures that synergistically combine the properties of dissimilar alloys. When there are different requirements for specific applications, bimetallic materials are used rather than a single material. Bimetallic materials, which integrate two different materials, offer a compelling solution by combining each material's excellent properties. For example, wear- and corrosion-resistant stainless steel can be combined with copper to enhance the heat conductivity of power plant boiler and gas turbine components [1]. In another application, SS316L-Ti64 bimetallic

structures can have very hard materials in the outer layers, providing excellent wear resistance, and inner material with excellent ductility and high toughness, where the parts are subjected to different load conditions [2]. Traditional joining and coating methods, such as welding [3], cold-sprayed coatings [4], thermally spraying [5], powder metallurgy [6], soldering, and interface diffusion [7], offer limited solutions with basic geometries to create bimetallics. Moreover, these methods face significant challenges in joining different materials due to their distinct thermal expansion coefficients, chemical incompatibility, and susceptibility to intermetallic phase formation at the interface [8-9]. Unlike the methods mentioned above, additive manufacturing

techniques have the unique capability of fabricating precisely controlled bimetallic components at complex geometry. Gurok et al. created bimetallic cutting tools using an additive manufacturing process with stainless steel and hard-facing materials, exhibiting good interfacial bonding, desirable microstructural features, and hardness gradient for wear-resistant applications [10].

Laser Directed Energy Deposition (L-DED) stands out as a leading additive manufacturing technology, offering the production of such complex multi-material systems [11]. In the L-DED process, a laser is employed to melt powder material as it is deposited onto a substrate. The powder material is fed through a nozzle, and the laser beam precisely melts and fuses it onto the substrate. L-DED exhibits versatility, as it can simultaneously use more than one raw material as feedstock, including metals, alloys, and ceramics. The selection of process parameters directly affecting the energy density delivered to the deposited material is crucial in L-DED. Improperly selected process parameters can lead to adverse thermally induced effects, such as lack of fusion, undesirable phase transformation, and excessive dilution [12]. Dilution, defined as the melting of the underlying material during deposition, can significantly influence interfacial integrity and mechanical properties. High energy densities can lead to a larger melt pool, potentially causing issues such as increased dilution and undesirable phase transformations due to excessive heat input, particularly in alloy systems prone to such effects [10]. Conversely, too low an energy density may result in insufficient melting of the material, manifesting as lack of fusion defects that can severely degrade the mechanical integrity of the build [13].

One of the most promising bimetallic structures is the combination of austenitic stainless steel SS316L and nickel-based superalloy IN718 [14-15]. SS316L offers excellent ductility, corrosion resistance, and cost-effectiveness [16], while IN718 exhibits high strength, hardness, and oxidation resistance at elevated temperatures [17]. The superior mechanical performance of IN718 is attributed to the solid solution-strengthening effects of elements such as Mo and Nb [18]. Despite the advantages of IN718, its higher cost motivates efforts to

selectively apply it only where high performance is required while using SS316L in less critical regions. Both alloys share a face-centered cubic (FCC) matrix structure (γ phase), predominantly alloyed with Fe, Cr, and Ni, facilitating their compatibility in layered deposition.

In this study, IN718 powder was deposited on SS316L substrates through L-DED in six different process conditions to examine the effect of energy density on interface geometry and dilution. The best combination of parameters was selected and utilized to build vertically deposited blocks of bimetallic SS316L-IN718 as well monolithic SS316L, monolithic IN718. The bimetallic samples were examined by line-EDS and Vickers micro-hardness profiling for determining the composition and hardness transition at the interface. Finally, we compared the tensile properties of monolithic alloys and bimetallic sample to evaluate bonding quality of the bimetal. The objective of this study is to establish a uniform process window for fabricating defect-free bimetallic components and to gain fundamental understanding for future mechanical performance evaluation.

2. MATERIAL AND METHOD

In this study, spherical IN718 and SS316L powder (45-153) produced via gas atomization was used as the feedstock material for L-DED processes. The chemical composition of the IN718 and SS316L powders is provided in Table 1. The deposition was fabricated using Erlaser Hard+Clad L-DED system, which has a diode laser (maximum power output of 4 kW) and a 6-axis Kuka robotic arm. Argon gas was used as both the shielding gas during the L-DED process to protect the molten material from oxidation and as a feeding gas. The focal length between the laser head and the part was maintained at 13 mm, resulting in a laser beam spot diameter of approximately 3.5 mm. The powder feed rate of 30 gr/min and the carrier gas flow of 15 L/min were kept constant during deposition. The study was conducted in two main stages. In the first stage, single wall bimetallic production was done by depositing IN718 powder over the wrought SS316L substrate under six different process parameter sets, as shown schematically in Figure 1 (a). In this stage, deposition was carried out in a single-track, multilayer configuration. Six wall

depositions were fabricated using varying combinations of laser power (1000, 1300, 1400W) and scan speed (11, 14 mm/s) to investigate the influence of energy density, calculated by Equation (1), on wall geometry, dilution at the interfacial zone, and deposition quality. The images of the produced single walls and the values of the parameters used for the process are shown in Figures 1(b) and (c), respectively. The ranges of parameters used for this stage were based on results from our preliminary tests. The linear energy density was calculated using the following expression:

$$\text{Energy density (J/mm)} = \frac{P}{V} \quad (1)$$

where P is laser power (W), and V is scan speed (mm/s). The optimal parameter set was identified based on optical microscope inspection. Before inspection, the samples were ground using SiC papers of 240-2500 grit size and polished using 6, 3, and 1 μm diamond solutions. Optical microscopy was employed to observe bonding geometry, microstructural features, and the presence of any defects such as porosity or cracks. The parametric set that exhibited optimal dilution [10] and stable geometries with no defect formation was selected as the optimum [19,20].

In the second stage of the study, bimetallic blocks were deposited entirely using L-DED, starting with SS316L powder and followed by IN718 powder. All blocks produced in this stage were fabricated with the same parameter set, which was selected as the optimal parameter set from single-wall productions. These blocks were used to investigate the bonding quality of SS316L-IN718 bimetallic interfaces through mechanical tests. Energy-Dispersive Spectroscopy (EDS) was utilized to verify bimetallic production through line elemental composition measurements. Vicker's microhardness measurements were performed using a 100 g force and a dwell time of 10 seconds with an AMH 55 (Leco Corporation, USA). In addition to bimetallic SS316L-IN718 blocks, monolithic form of SS316L and IN718 were produced to compare the tensile properties. Each block consisted of three vertically aligned tensile bars, fabricated with 110 layers to reach a total height of 82.5 mm, with a wall thickness of 6 mm and width of 50 mm, as shown in Figure 2. The geometries of the tensile specimens conformed to ASTM E8 standards, with a gauge length of 33 mm and a thickness of 2 mm (Figure 3). The tensile test was conducted at a constant strain rate of 0.015 mm/min using a Shimadzu Autograph 100 kN tensile test machine.

Table 1. Chemical composition (wt. %) of IN718 and SS316L powder

Material	Fe	Cr	Ni	Mn	Mo	Nb	Si	C	Co	Ti
SS316L	Bal.	17	12	2	2	-	0.1	0.03	-	-
IN718	Bal.	19	54	0.35	3	5	0.15	0.05	0.06	1

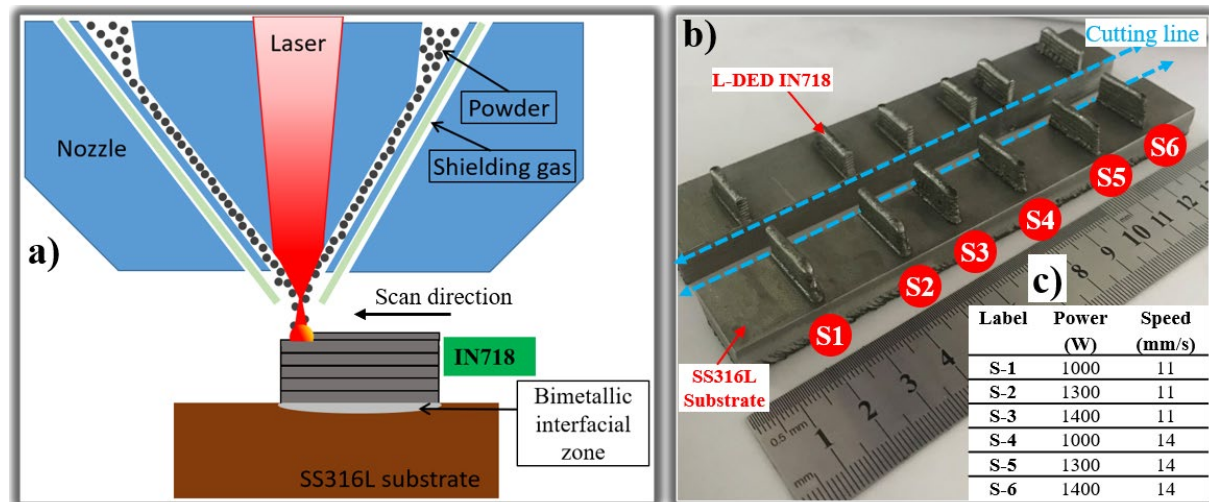


Figure 1. Single wall fabrication of IN718 on wrought SS316L substrate to form bimetallic interface via L-DED: (a) Schematic view of bimetal fabrication by IN718 deposition on wrought SS316L substrate, (b) Single wall depositions with different sets of parameters, which are cut with Electrical Discharge Machine (EDM) to inspect cross-section geometry, c) the process parameter matrix used for single wall depositions.

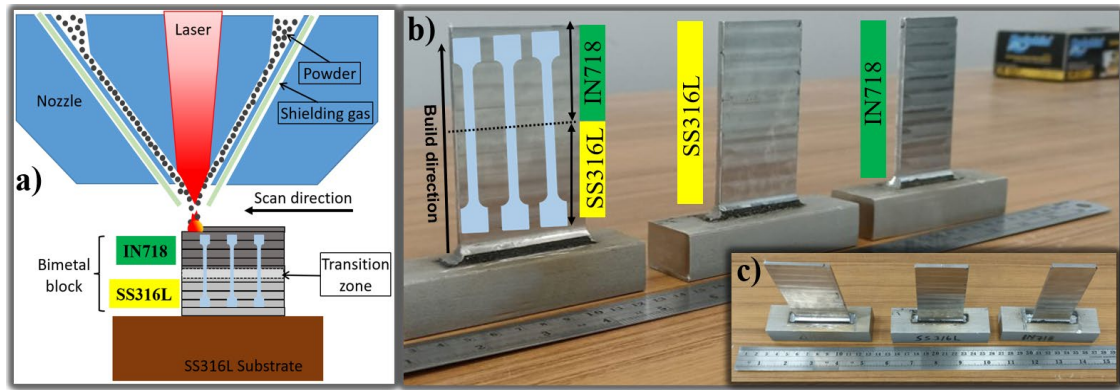


Figure 2. Vertical blocks fabrication in the form of IN718-SS316L bimetals via L-DED (a) Schematic view of bimetallic fabrication by IN718 deposition on L-DEDed SS316L, (b) front view of SS316L-IN718 bimetallic, and monolithic SS316L, IN718, (c) top view of SS316L-IN718 bimetallic, and monolithic SS316L, IN718.

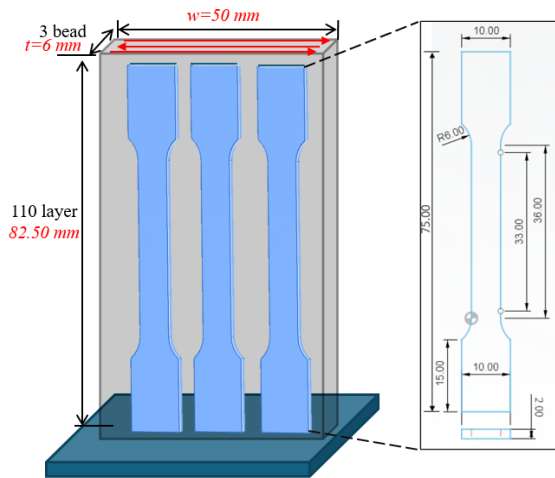


Figure 3. Schematic illustration of the vertical block fabricated via L-DED used for tensile specimen subtraction and test specimen geometry

3. RESULTS AND DISCUSSION

3.1. Single Wall Deposition

To investigate the effect of energy density on the interfacial quality and wall geometry of IN718 deposition on wrought SS316L substrate, single-wall depositions were performed using six different combinations of laser power and scan speed. The resulting energy densities ranged from 71.43 to 127.27 J/mm, as shown in Table 2. Cross-sectional views of the walls, including the interface area between IN718 deposition and SS316L substrate, were obtained by sectioning the samples perpendicular to the scanning direction. The penetration depth and width of the SS316L and IN718 interfaces were measured using ImageJ software applied to micrographs obtained from the optical microscope. The dilution ratio, which is a crucial parameter that determines the intermixing of materials at the interface, was calculated using Equation (2).

$$Dilution = \frac{D}{D+H} \quad (2)$$

where D is the penetration depth into the SS316L substrate and H is the height of the first layer of deposited IN718 above the substrate.

As depicted in Figure 4, the interface geometries were affected by the energy density values, leading to distinct dilution ratios. Higher energy density resulted in greater melting of the base material (SS316L), leading to increased mixing with the deposited material (IN718). The maximum dilution of 38.3% was observed in sample S-3, which had the highest energy density (127.27 J/mm), indicating significant substrate melting and mixing. In addition to increased dilution, excessively high energy densities can cause over melting, leading to unwanted changes in material properties and the vaporization of alloying elements [21]. Conversely, a lower energy density contributed to reduced dilution, resulting in less mixing of the base and deposited materials. The lowest dilution of 16.3% occurred in sample S-4, which had the lowest energy density (71.43 J/mm). However, relatively low energy density could result in insufficient fusion and the presence of unmelted powder near the interface, as shown in samples S-4 and S-5. This inadequate fusion increases the risk of defects, such as pores, which can have a detrimental impact on the mechanical properties and long-term performance of components. Maintaining a balanced energy density is essential for preventing both over-melting and lack of fusion defects. The energy density values between 90-100 J/mm resulted in an optimal balance

between dilution values of 18–20%, and defect-free deposition in agreement with the previous study by Kas et al. [22]. These values produced clean fusion zones without excessive melting of the base material, thereby preserving compositional gradients and minimizing the occurrence of fusion-induced fabrication defects.

In addition to dilution, the wall height and width of the IN718 deposition were evaluated to assess deposition quality, as shown in the optical microscope images in Figure 5. The highest wall height (8.96 mm) was achieved at sample S-1 with energy density of 90.91 J/mm,

producing a stable wall with good geometric integrity. The widest wall (2.8 mm) was achieved at sample S-3 with energy density of 127.27 J/mm. Although higher energy densities led to wider depositions, they also introduced potential issues such as melt pool instability and over-broadening of the deposited path [23]. The sample S-6 exhibited a good compromise between build height, dilution, and structural integrity. In particular, it resulted in a height of 8.3 mm, a width of 2.6 mm, and a dilution of 20.2%, with no signs of unmelted powder or porosity, demonstrating that it is the best parameter.

Table 2. Process parameters, energy density, wall height, width, and dilution results for single-wall depositions.

“	Power (W)	Speed (mm/s)	Energy Density (J/mm)	Height (mm)	Width (mm)	Dilution (%)
S-1	1000	11	90.91	8.96	2.65	18.4
S-2	1300	11	118.18	8.8	2.7	34
S-3	1400	11	127.27	8.7	2.8	38.3
S-4	1000	14	71.43	7.6	2.5	16.3
S-5	1300	14	92.86	7.9	2.55	19.3
S-6	1400	14	100	8.3	2.6	20.2

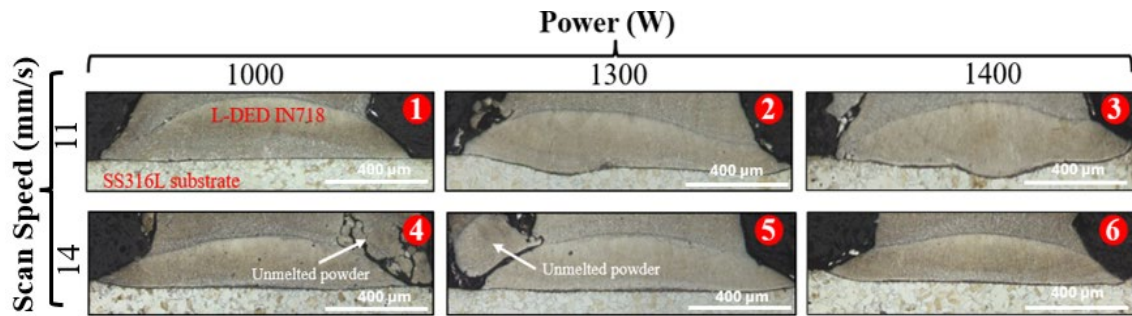


Figure 4. Cross-sectional OM images of the interfacial zone between IN718 deposition and wrought SS316L substrate were obtained at varying scan speeds and laser powers.

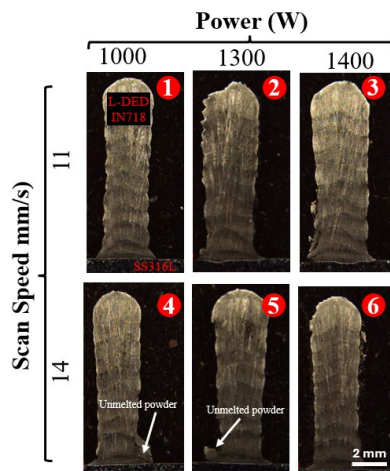


Figure 5. OM images of IN718 single-wall deposition fabricated on wrought SS316L substrate via L-DED, using varying scan speed and laser power.

3.2. Bimetallic Block Deposition

The mechanical and microstructural characterizations investigated in this section were performed on bimetallic and monolithic blocks fabricated using the process parameter set of sample S-6 (1400 W, 14 mm/s, 100 J/mm), which was identified as the optimal parameter set, as discussed in Section 3.1. The other parameter sets were excluded from further block fabrication due to observed issues such as excessive dilution, melt pool instability, or the presence of unmelted powder to save time and cost by prioritizing the most promising parameter set. Hence, further mechanical tests were conducted only for the optimal parameter set.

To investigate the composition change and elemental diffusion, the line EDS measurement was done on bimetallic SS316L-IN718 block. The line EDS result revealed a transition zone between the SS316L and IN718 materials, as shown in Figure 6. Specifically, a progressive decrease in Fe concentrations was observed in this region. Simultaneously, Ni, Nb, and Mo contents increased consistently, reflecting the compositional shift toward the IN718 alloy. This region spanned nearly 4 mm, corresponding to 5 to 6 deposited layers based on the layer thickness of 0.75 mm. Similarly, Grandhi et al. reported comparable elemental interdiffusion in cobalt-nickel bimetallic interfaces fabricated via L-DED, attributing this to convective flow within the melt pool [24]. The gradient structure between SS316L and IN718 is attributed not only to melt pool mixing and dilution during deposition but also potentially to the residual SS316L powder within the powder convey line, which was fed during the early stages of IN718 deposition.

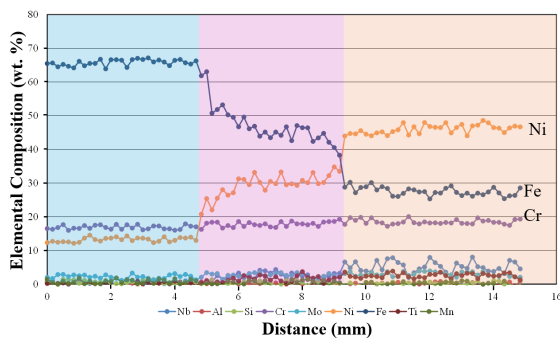


Figure 6. Elemental composition profile of the SS316L-IN718 bimetallic sample, which was obtained across the build direction.

Micro-hardness testing was performed across the interfaces from the SS316L region to the IN718 region to evaluate the hardness variations resulting from the composition change. The hardness profile along the cross-sections of the SS316L-IN718 interfaces was given in Figure 7. The hardness of the SS316L-IN718 bimetal exhibited a gradual increase across the interface, indicating that, despite the nominally abrupt change in material composition, substantial elemental interdiffusion took place at the interface during the deposition process. Ji et al. reported that a compositional diffusion across the interface facilitates a smoother transition, effectively minimizing stress concentrations that could otherwise degrade mechanical integrity and interfacial

performance [25]. The SS316L region exhibited hardness of 200-220 HV, consistent with its single-phase austenitic matrix. As the transition zone approached, a noticeable increase in hardness was observed, reflecting the change in composition. Within the transition zone, hardness values increased to 260-280 HV, highlighting the influence of alloying element interdiffusion and potential formation of fine secondary phases. The absence of abrupt hardness fluctuations across the transition zone suggests that the thermal profile induced by the selected process parameter set enabled gradual elemental diffusion while suppressing the formation of brittle intermetallic phases. The IN718 region exhibited the highest hardness values, ranging from 260 to 300 HV, which is typical for the as-deposited IN718 alloy due to solid solution and precipitation hardening of secondary phases.

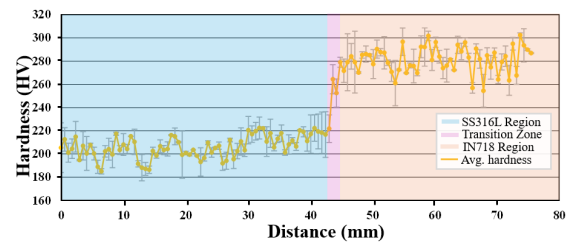


Figure 7. Hardness profile along the cross-section of the SS316L-IN718 bimetallic sample.

The mechanical properties of the SS316L-IN718 bimetallic interface were evaluated through tensile testing, and the results are presented in Figure 8. The monolithic counterparts of bimetal were also tested to compare the results.

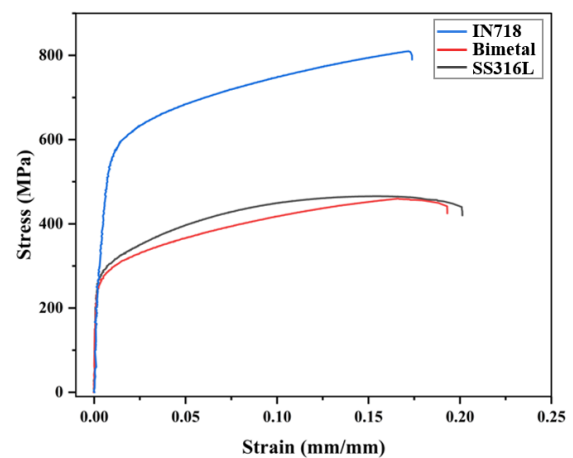


Figure 8. Stress-strain curves of SS316L, IN718, and SS316L-IN718 bimetallic specimens.

As shown in Table 3, the bimetallic sample exhibited a yield strength of 268.88 ± 20 MPa, a tensile strength of 462 ± 12 MPa, and an elongation of $19.6 \pm 0.8\%$. These values fall between those of SS316L and IN718, confirming the successful integration of the two dissimilar materials. Mechanical properties of the bimetallic sample were comparable to SS316L in terms of yield and ultimate strength, but with lower total elongation. The cause of the decrease in ductility was that half of the gauge length consisted of IN718, which has less inherent elongation capability compared to SS316L. The study by Lu et al. also showed elongation values between 16% and 21% for L-DED fabricated SS316L/IN718 functionally graded materials in the as-built and heat-treated conditions [26]. The necking and fracture occurred in the SS316L part of the bimetallic sample, indicating that the interface was stronger than the SS316L base alloy. The reason for the strong bonding between the parent alloys could be attributed to the gradual hardness transition and the absence of sharp compositional changes, which minimizes stress concentration at the interface. A ductile fracture mode was observed, with no signs of interfacial delamination or premature failure, validating the mechanical integrity of the bonding zone.

Table 3. Tensile properties of the bimetallic SS316L-IN718 sample and its parent alloy counterparts.

Sample	Yield Strength (MPa)	Tensile Strength (MPa)	Elong. (%)
Bimetal	268.88 ± 20	462 ± 12	19.6 ± 0.8
SS316L	280.5 ± 18	465 ± 15	20.8 ± 0.5
IN718	547.5 ± 13	820 ± 14	17.3 ± 0.7

4. CONCLUSION

In this study, SS316L-IN718 bimetallic structures were fabricated using L-DED by depositing IN718 on wrought SS316L and fully deposited SS316L-IN718 blocks. The effects of processing parameters on the interfacial quality and the mechanical performance of the bimetallic interface were investigated. In the first stage of the study, single wall depositions of IN718 on wrought SS316L were performed with various combinations of laser power and scan speed. The experimental results revealed that both dilution ratio at the interface and wall

geometry were significantly dominated by energy density. An optimum energy density range of 90–100 J/mm was established to achieve steady deposition with good bonding, regulated dilution (~18–20%), and least geometric distortion. In the second stage of the study, vertically built blocks were fabricated by using the parameter set of sample S-6 to inspect mechanical integrity and compare tensile properties of bimetallic samples with their monolithic counterparts. EDS line scanning along the SS316L-IN718 interface confirmed a smooth elemental transition over a 4 mm region. Micro-hardness measurements revealed a continuous transition from a hardness of ~210 HV in the SS316L region to a hardness of ~300 HV in the IN718 region without the presence of any defect-related degradation at the interface zone. Tensile testing revealed that the yield strength and ultimate strength of the bimetallic sample are 268.88 ± 20 MPa and 462 ± 12 MPa, respectively, in good agreement with SS316L. Elongation of bimetal is lower than SS316L but higher than IN718, and the fracture occurred on the SS316L side with noticeable necking and ductile behavior, demonstrating good interfacial bonding. The uniform hardness profile, absence of interface defects, and robust mechanical integrity confirm that the L-DED process can be used to fabricate functional SS316L-IN718 bimetallic components for structural applications.

ACKNOWLEDGES

This study was supported by the Scientific Research Projects Coordination Unit of Gazi University within the scope of the Priority Area Research Project, with the project number FOA-2023-8507.

REFERENCES

1. Kar, J., Roy, S.K., Roy, G.G., “Effect of beam oscillation on electron beam welding of copper with AISI-304 stainless steel”, *Journal of Material Processing Technology*, Vol. 223, Pages 174-185, 2016.
2. Alontseva, D., Yavuz, H.İ., Azamatov, B., Khoshnaw, F., Safarova, Y., Dogadkin, D., Avcu, E., Yamanoglu, R., “Improving corrosion and wear resistance of 316L stainless steel via in situ pure Ti and Ti6Al4V coatings: tribocorrosion and electrochemical analysis”, *Materials*, Vol. 18, Issue 3, Pages 553, 2025.

3. Sherpa, B.B., Rani, R., “Advancements in explosive welding process for bimetallic material joining: A review”, *Journal of Alloys and Metallurgical Systems*, Vol. 6, 2024.
4. Wu H., Xie, X., Liu, S., Xie, S., Huang, R., Verdy, C., Liu, M., Liao, H., Deng, S., Xie, Y., “Bonding behavior of bi-metal-deposits produced by hybrid cold spray additive manufacturing”, *Journal of Materials Processing Technology*, Vol. 299, 2022.
5. Singh, S., Berndt, C.C., Singh Raman, R.K., Singh, H., Ang, A.S.M., “Applications and developments of thermal spray coatings for the iron and steel industry”, *Materials*, Vol. 16, Issue 2, Page 516, 2023.
6. Chauhan, P. K., Khan, S., “Microstructural examination of aluminum-copper functionally graded material developed by powder metallurgy route”, *Materials Today: Proceedings*, Vol. 25, Issue 4, 2020.
7. Yilmaz, O., Çelik, H., “Electrical and thermal properties of the interface at diffusion-bonded and soldered 304 stainless steel and copper bimetal”, *Journal of Materials Processing Technology*, Vol. 141, Issue 1, Pages 67-76, 2003,
8. Wang, D., Liu, L., Deng, G., Deng, C., Bai, Y., Yang, Y., Han, C., “Recent progress on additive manufacturing of multi-material structures with laser powder bed fusion”, *Virtual and Physical Prototyping*, Vol. 17, Issue 2, Pages 329–365, 2022.
9. Bandyopadhyay, A., Zhang, Y., Onuik, B., “Additive manufacturing of bimetallic structures”, *Virtual and Physical Prototyping*, Vol. 17, Issue 2, Pages 256–294, 2022.
10. Dass, A., Moridi, A., “State of the art in directed energy deposition: From additive manufacturing to materials design”, *Coatings*, Vol. 9, Pages 415, 2019.
11. Gürol U., Dilibal S., Turgut B., Baykal H., Kümek H., Koçak M., “Manufacturing and characterization of WAAM-based bimetallic cutting equipment”, *International Journal of 3D Printing Technologies and Digital Industry*, Vol. 6, Issue 3, Pages 548-555, 2022.
12. Tan, Z. E., Pang, J. H. L., Kaminski, J., Pepin, H., “Characterization of porosity, density, and microstructure of directed energy deposited stainless steel AISI 316L”, *Additive Manufacturing*, Vol. 25, Pages 286-296, 2019.
13. Benarji, K., Kumar, Y., Paul, C., Jinoop, A., Bindra, K., “Parametric investigation and characterization on SS316 built by laser-assisted directed energy deposition”, *Proceedings of the Institution of Mechanical Engineers Part L Journal of Materials Design and Applications*, Vol. 234, Issue 3, Pages 452-466, 2019.
14. Mahmud, A., Ayers, N., Huynh, T., Sohn, Y., “Additive manufacturing of SS316/IN718 bimetallic structure via laser powder bed fusion”, *Materials*, Vol. 16, Issue 19, Page 6527, 2023.
15. Singh, S. P., Aggarwal, A., Upadhyay, R. K., Kumar, A., “Processing of IN718-SS316L bimetallic-structure using laser powder bed fusion technique”, *Materials and Manufacturing Processes*, Vol. 36, Issue 9, Pages 1028-1039, 2021.
16. Nouri, A., Wen, C., “Stainless steels in orthopedics”, In *Structural Biomaterials*, Pages 67-101, 2021.
17. Zhou, C., Wang, J., Hu, S., Tao, H., Fang, B., Long, L., Zhang, L., “Enhanced corrosion resistance of additively manufactured 316L stainless steel after heat treatment”, *Journal of the Electrochemical Society*, Vol. 167, Issue 14, Page 141504, 2020.
18. Vikram, R., Kirchner, A., Klöden, B., Suwas, S., “Optimized heat treatment for electron beam powder bed fusion processed IN718: correlating microstructure, texture, and mechanical properties”, *Advanced Engineering Materials*, Vol. 27, Issue 9, 2025.
19. Xu, J., Wu, Z., Niu, J., Song, Y., Liang, C., Yang, K., Chen, Y., Liu, Y., “Effect of laser energy density on the microstructure and microhardness of inconel 718 alloy fabricated by selective laser melting”, *Crystals*, Vol.12, Issue 9, Pages 2022.
20. Chen, Z., Sun, W., Huang, Y., Zhou, H., Yang, K., Lu, J., “The effect of laser energy density on microstructural evolution and mechanical properties of laser clad 316L stainless steel for repair”, *Surface and Coatings Technology*, Vol. 448, 2022.
21. Saboori, A., Aversa, A., Marchese, G., Biamino, S., Lombardi, M., Fino, P., “Application of directed energy deposition-based additive manufacturing in repair”, *Applied Sciences* Vol. 9, Issue 16, Page 3316, 2019.
22. Kas, M., Muslim, T., Yilmaz, O. Karagoz, T., Turedi, E., Gumus. S., Bayram, A., “Directed energy deposition of PH 13–8 Mo stainless steel: microstructure and mechanical property analysis”, *International Journal Advanced Manufacturing Technology*, Vol. 132, Pages 701–715, 2024.

23. Sampson, R., Lancaster, R., Sutcliffe, M., Carswell, D., Hauser, C., Barras, J., “The influence of key process parameters on melt pool geometry in direct energy deposition additive manufacturing systems”, *Optics & Laser Technology*, Vol. 134, 2021.
24. Grandhi, M., Nagaraj, A., Khosravi, H., Liu, Z., Min, S., “Mechanical and microstructural profiling of additively manufactured cobalt–nickel functional gradient structure”, *Manufacturing Letters*, Vol. 41, 2024.
25. Ji, C., Li, K., Zhan, J., Bai, S., Jiang, B., Murr, L. E., “The effects and utility of homogenization and thermodynamic modeling on microstructure and mechanical properties of SS316/IN718 functionally graded materials fabricated by laser-based directed energy deposition”, *Journal of Materials Processing Technology*, Vol. 319, 2023.
26. Lu, J., Li, W., “Improvement of tensile properties of laser directed energy deposited IN718/316L functionally graded material via different heat treatments”, *Materials Science and Engineering: A*, Vol. 866, 2023.